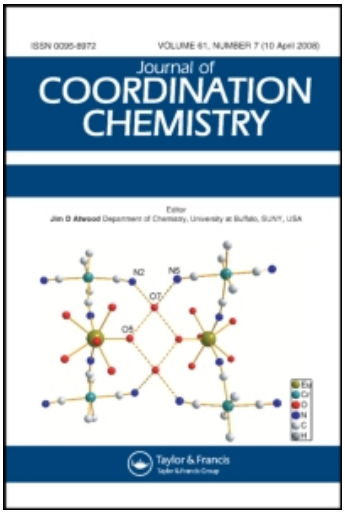

Journal of Coordination Chemistry
Publication details, including instructions for authors and subscription information:
http://www.informaworld.com/smpp/title~content=t713455674

Synthesis, crystal structure and magnetic properties of new Mn^{III}-Cu^{II} heterometallic aggregates based on multidentate Schiff-base ligands

Qiong Wu[a]; Quan Shi[a]; Yang-Guang Li[a]; En-Bo Wang[a]
[a] Department of Chemistry, Key Laboratory of Polyoxometalate Science of Ministry of Education, Northeast Normal University, Changchun, 130024, P.R. China

To cite this Article Wu, Qiong , Shi, Quan , Li, Yang-Guang and Wang, En-Bo(2008) 'Synthesis, crystal structure and magnetic properties of new Mn^{III}-Cu^{II} heterometallic aggregates based on multidentate Schiff-base ligands', Journal of Coordination Chemistry, 61: 19, 3080 — 3091
To link to this Article: DOI: 10.1080/00958970801998945
URL: http://dx.doi.org/10.1080/00958970801998945

Journal of Coordination Chemistry
Vol. 61, No. 19, 10 October 2008, 3080–3091

Taylor & Francis
Taylor & Francis Group

Synthesis, crystal structure and magnetic properties of new Mn^{III}–Cu^{II} heterometallic aggregates based on multidentate Schiff-base ligands

QIONG WU, QUAN SHI, YANG-GUANG LI* and EN-BO WANG*

Department of Chemistry, Key Laboratory of Polyoxometalate Science of Ministry of Education, Northeast Normal University, Changchun, 130024, P.R. China

(*Received 7 October 2007; in final form 10 January 2008*)

Reaction of copper powder, manganese(II) nitrates and multidentate Schiff-base ligands in hot methanol solution led to the isolation of two new Mn^{III}–Cu^{II} heterometallic aggregates, $[Mn_2^{III}Cu_2^{II}(H_2L)_4]\cdot(NO_3)_2\cdot 2CH_3OH$ (**1**) (H_4L=2-[(2-hydroxy-benzylidene)-amino]-2-hydroxymethyl-proane-1,3-diol) and $[Mn^{III}Cu^{II}{}_3(sae)_4(MeOH)(H_2O)_3]\cdot NO_3\cdot MeOH$ (**2**) (H_2sae = salicylidene-2-ethanolamine). Both compounds were characterized by elemental analysis, IR, XPS, EPR, XRPD and single crystal X-ray diffraction. Compound **1** crystallizes in the triclinic space group $P\bar{1}$ with $a=11.1268(4)$ Å, $b=11.6153(4)$ Å, $c=11.8129(5)$ Å, $\alpha=88.435(10)^\circ$, $\beta=80.203(10)^\circ$, $\gamma=77.572(10)^\circ$, $V=1469.13(10)$ Å^3, $Z=1$, $R1(wR2)=0.0300(0.0771)$. Compound **2** crystallizes in the monoclinic space group $P2_1/n$ with $a=18.1715(7)$, $b=12.9931(5)$, $c=19.5903(8)$ Å, $\beta=97.1980(10)^\circ$, $V=4588.9(3)$ Å^3, $Z=4$, $R1(wR2)=0.0667$ (0.1998). The magnetic susceptibilities of **1** and **2** display the antiferromagnetic interactions in both compounds.

Keywords: Heterometallic aggregates; Schiff-base ligand; Zerovalent copper; Magnetism

1. Introduction

Interest in the design and synthesis of polynuclear transition metal aggregates originates from their tunable magnetic properties [1] and structural relevance to bioinorganic areas [2]. In this field, heterometallic manganese clusters have been paid much attention owing to their remarkable catalytic ability and properties as single-molecule magnets (SMM) [3–5]. Use of suitable multidentate N– and O–donor ligands has been effective for isolation of heterometallic manganese clusters based on carboxylato–, oxo–, and alkoxo-bridges, exhibiting a variety of structural topologies [3–10]. The employment of polydentate Schiff-base ligands, which can both chelate and bridge metal ions, represents a promising route to the synthesis of new heterometallic complexes (see scheme 1) [4, 5]. A number of heterometallic aggregates have been synthesized

*Corresponding authors. Email: wangenbo@public.cc.jl.cn (E.B. Wang); wangeb889@nenu.edu.cn (E.B. Wang); liyg658@nenu.edu.cn (Y.G. Li)

ISSN 0095-8972 print/ISSN 1029-0389 online © 2008 Taylor & Francis
DOI: 10.1080/00958970801998945

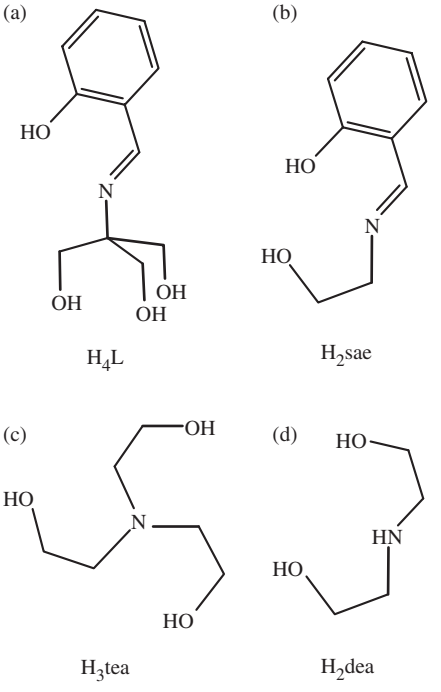

Scheme 1. Schematic view of the structures of Schiff-base ligands and aminoalcohol ligands: (a) H_4L (2-[(2-hydroxy-benzylidene)-amino]-2-hydroxymethyl-proane-1,3-diol); (b) H_2sae (salicylidene-2-ethanolamine); (c) H_3tea (triethanolamine); (d) H_2dea (diethanolamine).

by mixture of two kinds of transition metal salts and various Schiff-base ligands in a one-pot reaction system [4]. However, the reaction between two mixed transition metal ions and the Schiff-base ligand in one system always led to isolation of monometallic complexes mixed together or just one kind of monometallic aggregate. A more feasible synthetic route to heterometallic systems is step-by-step reaction of different metal ions with ligands that have multi-coordination sites, with different affinity of metal ions [5–8]. A recent advance in this field indicates that new heterometallic aggregates could be synthesized by reaction between zerovalent copper and various transition metal salts and aminoalcohols in organic solvents, presenting a more effective method for new heterometallic compounds [9]. A series of new heterometallic Cu–M ($M = Co^{II}$, Zn^{II}, Cd^{II}, Pd^{II}, Mn^{III}) compounds have been reported [9, 10]. Considering the structural similarity between aminoalcohols and the Schiff-base ligands (see scheme 1), we introduce various Schiff-base ligands into such a synthetic route so as to explore new Mn^{III}–Cu^{II} heterometallic aggregates. Herein, we report two such compounds, $[Mn_2{}^{III}Cu_2{}^{II}(H_2L)_4] \cdot (NO_3)_2 \cdot 2CH_3OH$ (**1**) (H_4L=2-[(2-hydroxy-benzylidene)-amino]-2-hydroxymethyl-proane-1,3-diol) and $[Mn^{III}Cu^{II}{}_3(sae)_4(MeOH)(H_2O)_3] \cdot NO_3 \cdot MeOH$ (**2**) (H_2sae = salicylidene-2-ethanolamine). Compound **1** exhibits a dicubane-like $\{Cu^{II}{}_2Mn^{III}{}_2\}$ tetranuclear cluster surrounded by four pentadentate Schiff-base ligands. Compound **2** shows a cubane-like $\{Cu^{II}{}_3Mn^{III}\}$ tetranuclear cluster coordinated by four tri-dentate Schiff-base ligands. The magnetic properties of **1** and **2** were investigated.

2. Experimental

2.1. *Materials and methods*

All chemicals purchased were of reagent grade and used without further purification. Elemental analyses (C, H, N) were performed on a Perkin–Elmer 2400 CHN elemental analyzer. Mn and Cu were determined by a Leaman inductively coupled plasma (ICP) spectrometer. IR spectra were recorded in the range 400–4000 cm^{-1} on an Alpha Centauri FT/IR spectrophotometer with pressed KBr pellets. XPS analyses were performed on a VG ESCALABMKII spectrometer with a Mg-Kα (1253.6 eV) achromatic X-ray source. The vacuum inside the analysis chamber was maintained at 6.2×10^6 Pa during the analysis. EPR spectra were obtained on a Japanese JES-FE3AX spectrometer at 77 K. X-ray powder diffraction (XRPD) studies were performed with a NETZSCH STA 449C instrument, with a Panalytical X-Pert pro diffractometer with Cu-Kα radiation. The variable-temperature solid state magnetic susceptibilities (χ_M) were measured with a Quantum Design MPMS7 SQUID magnetometer at a 0.1 T dc field in the temperature range 2–300 K. Diamagnetic corrections were made with Pascal's constants [11].

2.2. *Synthesis of* $[Mn_2^{III}Cu_2^{II}(H_2L)_4]\cdot(NO_3)_2\cdot 2CH_3OH$ *(1)*

Salicylaldehyde (0.122 g, 1.0 mmol), tris(hydroxymethyl)aminomethane (0.121 g, 1.0 mmol) and triethylamine (0.101 g, 1.0 mmol) were dissolved in methanol (25 mL), forming a yellow solution. Then, $Mn(NO_3)_2\cdot 6H_2O$ (0.144 g, 0.5 mmol) and copper powder (0.032 g, 0.5 mmol) were successively added to the solution with stirring. The yellow suspension was heated at 65°C for 4 h and slowly changed to a brown solution during this time. After filtration, the brown filtrate was sealed in a beaker and kept undisturbed at room temperature. Dark-green block crystals of 1 were isolated after one week (Yield: 75% based on Mn). Elemental analysis for $C_{48}H_{68}N_6O_{26}Cu_2Mn_2$ ($M_r = 1382.05$) 1 (%): Calcd C, 41.71; H, 4.96; N, 6.08; Mn, 7.95; Cu, 9.20. Found: C, 42.76; H, 4.87; N, 6.14; Mn, 8.13; Cu, 9.31. Selected IR (KBr pellet, cm^{-1}): 3270(s), 2931(s), 2873(s), 1602(s), 1543(s), 1476(s), 1442(s), 1374(s), 1298(s), 1204(s), 1154(s), 1043(s), 1010(w), 908(m), 832(w), 755(s), 679(w), 629(m), 552(s), 501(m), 459(s).

2.3. *Synthesis of* $[Mn^{III}Cu^{II}_3(sae)_4(MeOH)(H_2O)_3]\cdot NO_3\cdot MeOH$ *(2)*

Salicylaldehyde (0.122 g, 1.0 mmol), ethanolamine (0.061 g, 1.0 mmol) and triethylamine (0.101 g, 1.0 mmol) were dissolved in methanol (25 mL), forming a yellow solution. To this solution was successively added $Mn(NO_3)_2\cdot 6H_2O$ (0.144 g, 0.5 mmol) and copper powder (0.032 g, 0.5 mmol) with stirring at 65°C for 4 h. After cooling to room temperature, the final dark brown solution was filtered and the filtrate was sealed in a beaker undisturbed at room temperature. Dark-green block crystals of **2** were isolated in one week (Yield: 50% based on Mn). Elemental analysis for $C_{38}H_{50}N_5O_{16}Cu_3Mn$ ($M_r = 1078.40$) **2** (%): Calcd C, 42.32; H, 4.67; N, 6.49; Mn, 5.09; Cu, 17.68. Found: C, 42.39; H, 4.59; N, 6.55; Mn, 5.17; Cu, 17.74. Selected IR (KBr pellet, cm^{-1}): 3376(br), 2931(w), 1645(s), 1543(s), 1450(s), 1382(w), 1289(sh), 1188(s), 1162(s), 1035(s), 942(s), 891(s), 857(w), 755(s), 645(s), 595(s), 527(m), 476(m), 442(m).

Table 1. Crystal data and structure refinement for **1** and **2**.

	1	**2**
Empirical formula	$C_{48}H_{68}N_6O_{26}Cu_2Mn_2$	$C_{38}H_{50}N_5O_{16}Cu_3Mn$
Formula weight	1382.04	1078.39
Temperature (K)	150(2)	150(2)
Wavelength (Å)	0.71073	0.71073
Crystal system	Triclinic	Monoclinic
Space group	$P\bar{1}$	P2(1)/n
a (Å)	11.1268(4)	18.1715(7)
b (Å)	11.6153(4)	12.9931(5)
c (Å)	11.8129(5)	19.5903(8)
α (°)	88.435(10)	
β (°)	80.203(10)	97.198(10)
γ (°)	77.572(10)	
V (Å^3)	1469.13(10)	4588.9(3)
Z	1	4
D_{Calcd} (g cm^3)	1.562	1.561
Absorption coefficient (mm^{-1})	1.222	1.712
F(000)	714	2212
Reflections collected/unique	8315/5079 [R(int) = 0.0167]	24871/7905 [R(int) = 0.0435]
Completeness to $\theta = 25.00$	98.4%	97.8%
Data/restraints/parameters	5079/18/397	7905/34/535
Goodness-of-fit on F^2	1.013	1.185
Final R indices [$I > 2\sigma(I)$]	$R1 = 0.0300$, $wR2 = 0.0734$	$R1 = 0.0667$, $wR2 = 0.1808$
R indices (all data)	$R1 = 0.0360$, $wR2 = 0.0771$	$R1 = 0.0948$, $wR2 = 0.1998$
Largest diff. peak and hole (e A^{-3})	0.486 and −0.328	1.759 and −1.600

[a] $R_1 = \Sigma F_o\| - |F_c\|/\Sigma|F_o|$; [b] $wR_2 = \Sigma[w(F_o^2 - F_c^2)^2]/\Sigma[w(F_o^2)^2]^{1/2}$.

2.4. *X-ray crystallography*

A suitable single crystal was glued at the end of a glass capillary. The data were collected on a Rigaku R-AXIS RAPID IP diffractometer with Mo-Kα (λ = 0.71073 Å) operating at 150 K. Empirical absorption corrections were applied. The structures of **1** and **2** were solved by the direct method and refined by full-matrix least-squares on F^2 using the SHELXL 97 software [12]. During refinement, all non-hydrogen atoms in **1** were refined anisotropically. The hydrogen atoms on carbon were fixed in calculated positions. In **2**, all the non-H atoms were refined anisotropically except the NO_3^- and methanol. The NO_3^- and methanol exhibit unreasonable thermal factors (Ueq) with the anisotropic refinement parameters; thus, they were refined isotropically. All H atoms on carbon were fixed in calculated positions. The H atoms on aqua ligands can not be found in residual electron density maps and directly included in the final molecular formula. A summary of the crystallographic data and structural determination for **1** and **2** is provided in table 1. Selected bond lengths and angles of **1** and **2** are listed in tables 2 and 3, respectively.

3. Results and discussion

3.1. *Synthesis*

The reaction of zerovalent copper with bivalent transition metal salts and aminoalcohols has proved effective for preparation of heterometallic aggregates [9],

Table 2. Selected bond lengths (Å) and angles (°) of **1**.

Cu(1)–N(1)	1.9140(19)	Mn(1)–O(5)	1.8627(16)
Cu(1)–O(1)	1.9326(16)	Mn(1)–O(6)	1.9160(15)
Cu(1)–O(6A)	1.9680(15)	Mn(1)–O(2)	1.9404(15)
Cu(1)–O(2)	1.9885(16)	Mn(1)–N(2)	1.9920(19)
Cu(1)–O(7A)	2.3720(17)	Mn(1)–O(1A)	2.2294(16)
Cu(1)–O(6)	2.4023(15)	Mn(1)–O(3)	2.3037(16)
Cu(1)···Mn(1[a])	3.0643(4)	Cu(1)···Mn(1)	3.1033(4)
N(1)–Cu(1)–O(6)	100.05(7)	O(5)–Mn(1)–O(6)	173.66(7)
O(1)–Cu(1)–O(6)	92.12(6)	O(6)–Mn(1)–O(2)	88.67(6)
O(6A)–Cu(1)–O(6)	80.69(6)	O(6)–Mn(1)–N(2)	81.38(7)
O(2)–Cu(1)–O(6)	75.07(6)	O(6)–Mn(1)–O(1A)	77.47(6)
O(7A)–Cu(1)–O(6)	168.35(5)	O(6)–Mn(1)–O(3)	92.50(6)
O(6A)–Cu(1)–O(7A)	88.17(6)	O(1[a])–Mn(1)–O(3)	169.97(6)
Mn(1)–O(6)–Cu(1A)	104.17(7)	Mn(1)–O(6)–Cu(1)	91.17(6)
Mn(1)–O(2)–Cu(1)	104.34(7)	Cu(1)–O(1)–Mn(1A)	94.56(6)
Cu(1 A)–O(6)–Cu(1)	99.31(6)		

Symmetry transformations used to generate equivalent atoms: A $-x, -y, -z$.

Table 3. Selected bond lengths (Å) and angles (°) of **2**.

M (1)–O(1)	1.900(4)	M(2)–O(3)	1.891(4)
M (1)–N(1)	1.943(5)	M(2)–N(2)	1.922(5)
M (1)–O(6)	1.953(4)	M(2)–O(4)	1.953(4)
M (1)–O(2)	1.967(4)	M(2)–O(2)	1.961(4)
M(1)–O(8)	2.527(4)	M(2)–O(10)	2.435(10)
M(1)–O(9)	2.483(5)	M(2)–O(6)	2.485(4)
M(3)–O(5)	1.902(4)	M(4)–O(7)	1.883(5)
M(3)–N(3)	1.936(5)	M(4)–N(4)	1.940(5)
M(3)–O(8)	1.944(4)	M(4)–O(8)	1.946(4)
M(3)–O(6)	1.962(4)	M(4)–O(4)	1.968(4)
M(3)–O(11)	2.375(5)	M(4)–O(12)	2.391(7)
M(3)–O(4)	2.505(4)	M(4)–O(2)	2.451(4)
O(1)–M(1)–O(2)	170.55(18)	O(3)–M(2)–O(4)	175.3(2)
N(1)–M(1)–O(2)	84.3(2)	N(2)–M(2)–O(4)	84.3(2)
O(6)–M(1)–O(2)	88.47(18)	O(4)–M(2)–O(2)	86.97(17)
O(8)–M(1)–O(2)	76.89(14)	O(4)–M(2)–O(10)	86.9(3)
O(9)–M(1)–O(2)	89.65(16)	O(6)–M(2)–O(4)	77.74(14)
O(5)–M(3)–O(6)	170.17(19)	O(7)–M(4)–O(8)	176.08(19)
N(3)–M(3)–O(6)	83.65(19)	N(4)–M(4)–O(8)	83.93(19)
O(8)–M(3)–O(6)	88.17(17)	O(8)–M(4)–O(4)	87.35(18)
O(6)–M(3)–O(11)	91.01(18)	O(8)–M(4)–O(12)	88.4(2)
O(6)–M(3)–O(4)	77.12(14)	O(2)–M(4)–O(8)	79.20(15)
M(1)–O(2)–M(2)	104.73(18)	M(1)–O(8)–M(4)	100.91(16)
M(1)–O(6)–M(2)	88.19(14)	M(1)–O(2)–M(4)	102.86(16)
M(1)–O(6)–M(3)	107.00(18)	M(2)–O(6)–Mn(3)	102.74(15)
M(1)–O(8)–M(3)	88.42(14)	M(2)–O(4)–Mn(3)	102.27(15)
M(2)–O(2)–M(4)	89.97(14)	M(3)–O(4)–M(4)	88.55(14)
M(2)–O(4)–M(4)	106.28(18)	M(3)–O(8)–M(4)	107.99(19)

especially Mn^{III}–Cu^{II} clusters [10]. Various aminoalcohols such as triethanolamine (H_3tea) and diethanolamine (H_2dea) act as proton donating agents [9a] for oxidation of copper and bivalent transition metal ions in air and also as multidentate ligands that can assemble various metal centers into heterometallic clusters [9, 10]. Schiff-base ligands exhibit similar structural features to aminoalcohols except the phenoxy

groups (see scheme 1). Thus, Schiff-base ligands could substitute for aminoalcohols in this reaction system. In our experiments, two multidentate Schiff-base ligands were prepared *in situ* in methanol and reacted with zerovalent copper and manganese nitrates, leading to isolation of **1** and **2**. During the synthesis, copper powder was slowly dissolved into the hot methanol solution and the initial yellow suspension slowly changed into a dark brown solution. In the final compounds, all Cu^0 was oxidized into Cu^{2+} and all Mn^{2+} was oxidized to Mn^{3+}, as shown in equations (1) and (2).

$$2Cu^0 + 2Mn(NO_3)_2 + 4H_4L + 1.5O_2 + 2TEA + 2MeOH \rightarrow [Mn_2^{III}Cu_2^{II}(H_2L)_4] \cdot (NO_3)_2 \cdot 2MeOH + 3H_2O + 2TEA \cdot HNO_3 \quad (1)$$

$$3Cu^0 + Mn(NO_3)_2 + 4H_2L + 1.75O_2 + TEA + 2MeOH \rightarrow [Mn^{III}Cu_3^{II}(sae)_4(MeOH)(H_2O)3] \cdot (NO_3) \cdot MeOH + 0.5H_2O + TEA \cdot HNO_3 \quad (2)$$

3.2. *Crystal structures*

Compound **1** crystallizes in triclinic space group $P\bar{1}$. The core of **1**, as shown in figure 1 and figure S1, exhibits a centrosymmetric dicubane-like $\{Cu_2Mn_2\}$ unit. Two Cu centers lie in the inner part while two Mn centers reside in the outer part. Each Cu center is six-coordinate, linking with five O atoms and one N atom derived from three different H_2L^{2-} ligands. The bond lengths of Cu–O(N) are in the range 1.9140(2) ~ 2.4023(2) Å, and the bond angles of O(N)–Cu–O vary from 75.07(6) to 168.35(5)°. Both Mn centers display six-coordinate octahedral geometry, with five O atoms and one N atom from three different H_2L^{2-} ligands. The Mn–O and Mn–N bond lengths are in the range 1.8627(2) ~ 2.3037(2) Å, and the bond angles of O(N)–Mn–O vary from 77.47(6) to 173.66(7)°. The oxidation states of Cu and Mn can be assigned as Cu^{II} and Mn^{III} based on charge-balance consideration, bond-valence sum calculations [13] and the presence of Mn centers with Jahn-Teller elongation axes (see figure 1).

In **1**, H_4L contains one phenoxy and three alkoxy groups and are partially deprotonated to H_2L^{2-}, adopting two coordination modes. Two contain one μ_3-alkoxy

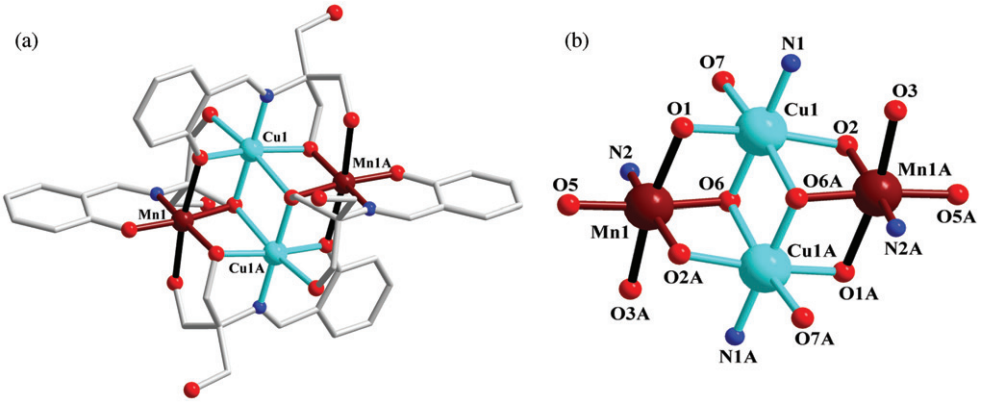

Figure 1. (a) Ball-and-stick view of the cationic cluster of **1**; (b) The tetranuclear core of **1** showing the coordination modes of Cu and Mn centers. Color code online: Cyan ball, Cu; Brown ball, Mn; Red ball, O; Blue ball, N; Grey line: H_2L^{2-} ligand.

linked with one Mn and two Cu centers. Another alkoxy arm is terminally coordinated with Cu. The remaining alkoxy is protonated. The association of phenoxy and the N-donor site functions as a bidentate chelate ligand to stabilize the Mn centers. The other two H_2L^{2-} ligands contain one μ_2-alkoxy linked with one Mn and Cu center. Another alkoxy is a terminal oxygen ligand coordinated to a Mn. The other alkoxy group is protonated. The phenoxy group associated with the N-donor ligand functions as a bidentate chelate ligand to stabilize the Cu centers. Further, the phenoxy group also acts as a μ_2-bridge to join Cu and Mn. Compound **1** represents a new example of heterometallic aggregates based on such a pentadentate Schiff-base ligand.

In the unit cell, the cationic cluster is charged-balanced by two NO_3^- anions. In the packing arrangement, the clusters are well separated (see figure 2 and figure S2) with extensive weak H-bonding interactions among the cationic clusters, NO_3^- and solvent methanol molecules. The typical H-bonds in **1** are listed in table 4.

Compound **2** crystallizes in the monoclinic space group $P2_1/n$. The unit cell of **2** contains one cationic heterometallic cluster, a NO_3^- and a methanol. The core of **2** exhibits a cubane-like $\{Cu_3Mn\}$ unit as shown in figure 3 and S3. All metal centers exhibit site-occupancy disorder with 75% Cu and 25% Mn occupancy in each site. The metal centers are six-coordinate with one N and four O donors from three different sae^{2-} ligands and O ligands from aqua or methanol. The bond lengths of MO–(N) are in the range $1.883(5) \sim 2.527(4)$ Å, and the bond angles of O(N)–M–O vary from $76.89(1) \sim 176.08(2)^\circ$. All the oxidation states of Cu and Mn are assigned to +2 and +3 based on the deep-blue crystal color, charge-balance consideration and the bond-valence sum calculation [13].

In **2**, all four H_2sae ligands are deprotonated into sae^{2-} and exhibit the same coordination mode. The alkoxy group in the sae^{2-} is a μ_3-bridge joining three metal centers. The phenoxy group associated with the N-donor functions as a bidentate chelate to stabilize the metal centers. The aqua or solvent methanol is a terminal ligand to fulfill the six-coordinate environment of all metal centers. Such an octahedral

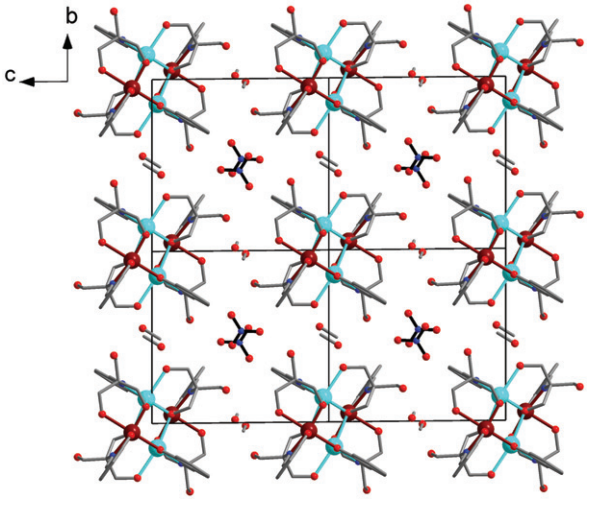

Figure 2. The packing arrangement of **1** viewed along the *a* axis.

Table 4. Typical H-bonding interactions in **1**.

O···H–X	O···X (Å)	O···H (Å)	H–X (Å)	Angle (°)
O9···H8–O8	2.727(3)	1.929(2)	0.813(2)	172.10(2)
O10···H16A–C16	3.492(4)	2.581(2)	0.990(3)	160.79(2)
O11···H18A–C18	3.253(4)	2.339(2)	0.990(2)	161.11(2)
O13···H7–O7	2.729(3)	1.937(2)	0.820(2)	162.10(2)
O12···H8–O8	2.700(3)	1.893(2)	0.810(2)	173.85(2)

Symmetry: $x, -y, 1-z$; $1-x, -y, 1-z$; $x, 1+y, z$; x, y, z; x, y, z.

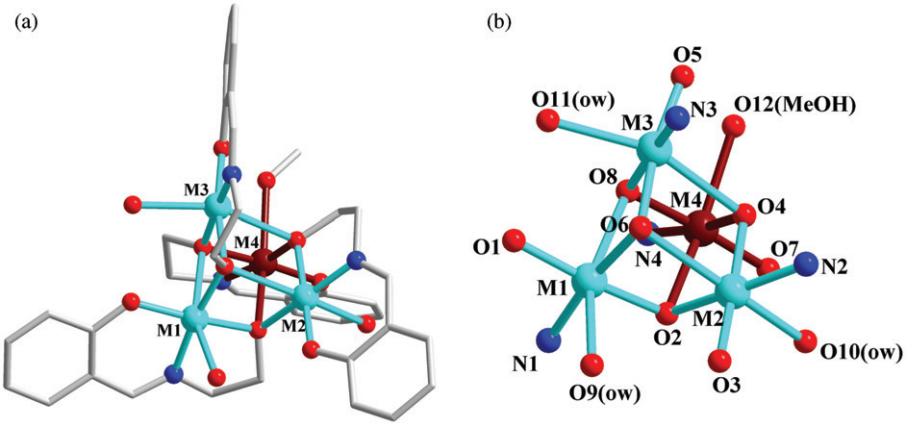

Figure 3. (a) Ball-and-stick view of the cationic cluster of **2**; (b) The tetranuclear core of **2**. All the metal centers (M) possess site occupancy disorder with 3/4 Cu and 1/4 Mn occupancies in each M site. Color code online: Cyan ball, Cu; Brown ball, Mn; Red ball, O; Blue ball, N; Grey line: sae^{2-} ligand.

coordination geometry on metal centers has rarely been observed in Cu-containing cubane-like clusters [14]. In the packing arrangement, all the cationic clusters are well separated (see figure 4 and figure S4) with extensive H-bonding interactions among cationic clusters, NO_3^- counter-anions and methanol, which stabilize the whole crystal structure. The typical H-bonds of **2** are listed in table 5.

3.3. *XPS and EPR spectra*

The oxidation states of Cu and Mn in **1** and **2** are further confirmed by XPS and EPR measurements. The XPS spectra were carried out in the energy region of Mn $2p_{3/2}$ and Cu $2p_{3/2}$, respectively. The peaks at 641.3 eV and 931.6 eV are ascribed to Mn^{3+} and Cu^{2+} ions, respectively (see figure 5) [15]. Further, the peak distances between $2p_{3/2}$ and $2p_{1/2}$ are 11.3 eV for Mn^{3+} and 19.8 eV for Cu^{2+}, in good agreement with reported results [15]. The EPR spectra of **1** and **2** at 77 K only show Cu^{2+} signals with average $g = 2.02$ and $g = 1.90$, respectively (see figure 6). The Mn^{III} signals are too weak or concealed by the strong and broad peaks of Cu^{2+}. The XPS and EPR results agree with the BVS calculation, further confirming the oxidation states of Cu^{2+} and Mn^{3+} in both compounds.

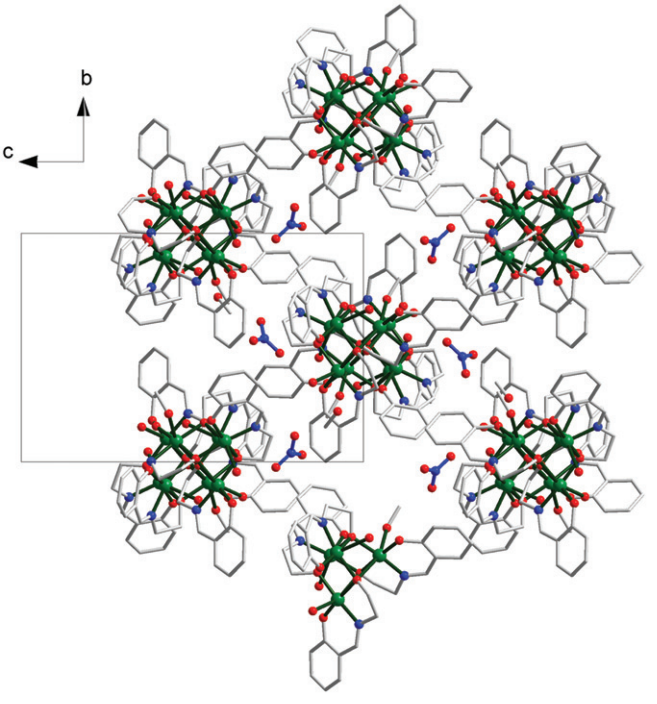

Figure 4. The packing arrangement of **2** viewed along the *a* axis.

Table 5. Typical H-bonding interactions in **2**.

O···H–X	O···X	O···H	H–X	Angle
O15···O11(OW)	2.796(1)			
O16···H26A–C26	3.548(2)	2.865(1)	0.969(6)	128.31(5)
O17···H34–C34	3.592(1)	2.689(1)	0.930(7)	163.81(5)
O13···O9(OW)	2.932(1)			

Symmetry: x, y, z; x, y, z; $-x, 1-y, -z$; $1/2-x, 1/2+y, 1/2-z$.

3.4. *X-ray powder diffraction for 1 and 2*

To check the phase purity of **1** and **2**, X-ray powder diffraction of both compounds was checked at room temperature. As shown in figure 7, the peak positions of simulated and experimental XRPD patterns are in agreement with each other, indicating good phase purity of the compounds. The differences in intensity may be due to the preferred orientation of the crystalline powder samples.

3.5. *Magnetic properties for 1 and 2*

The magnetic susceptibilities of **1** and **2** were measured with polycrystalline samples at 0.1 T in the temperature range 2–300 K. The thermal variation of the χT product of **1** is shown in figure 8(a). At 300 K, χT is 5.5 $cm^3\,K\,mol^{-1}$ and slowly decreases to 4.0 $cm^3\,K\,mol^{-1}$ at 50 K. Below this temperature, the χT value grows to the maximum

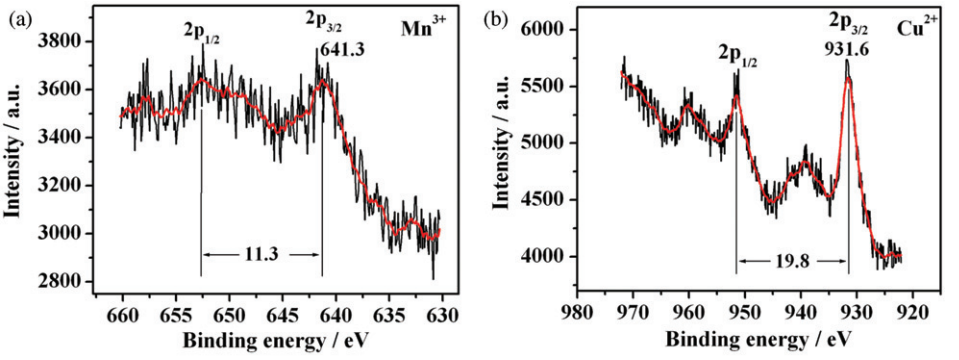

Figure 5. The XPS spectra of **1**.

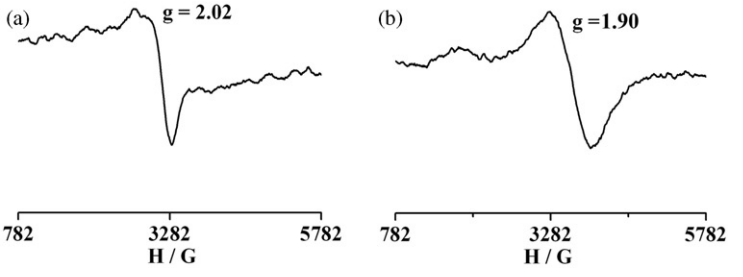

Figure 6. EPR spectra of **1 (a)** and **2 (b)**.

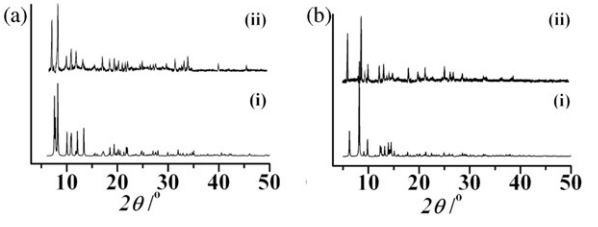

Figure 7. Simulated and experimental XRPD patterns of **1** (a) and **2** (b). In each plot, (i) is the simulated XRPD and (ii) is the experimental XRPD at room temperature.

of $4.9\,cm^3\,K\,mol^{-1}$ at 20 K, and then rapidly drops to $4.1\,cm^3\,K\,mol^{-1}$ at 2 K. The magnetic susceptibilities of **1** obey the Curie-Weiss law in the temperature range of 50–300 K (as shown in figure 8(a) insert plot). The Curie constant $C = 5.75\,cm^3\,K\,mol^{-1}$ is in agreement with the spin only value for magnetically isolated Mn^{III} and Cu^{II} ions ($6.75\,cm^3\,K\,mol^{-1}$, $g = 2$). The negative Weiss constant $\theta = -25.5\,K$ indicates the presence of an overall antiferromagnetic interaction in **1**. The decrease of χT below 20 K may be due to the saturation effect and zero-field-splitting (ZFS) of Mn^{III} ions. Trying to fit the susceptibility data of **1** with a simple butterfly model failed, probably due to the simple model.

The χT *versus* T plot of **2** is shown in figure 8(b). The χT is equal to $3.4\,cm^3\,K\,mol^{-1}$ at 300 K, a little lower than expected for magnetically isolated Mn^{III} and Cu^{II} ions

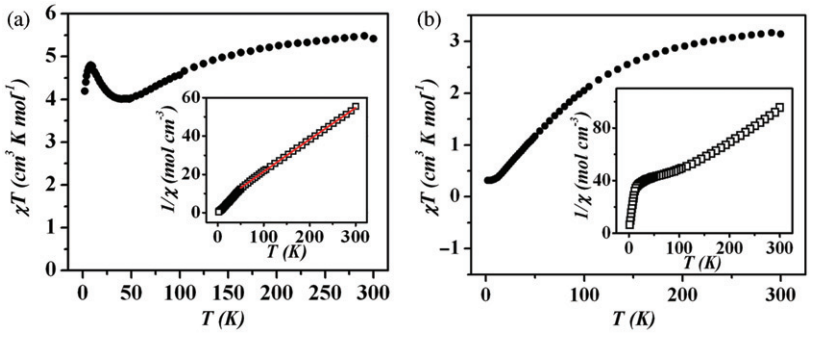

Figure 8. χT *vs.* T curves of **1** (a) and **2** (b). (insert: $1/\chi$ *vs.* T curve. The red line (online) is the fitting curve of Curie-Weiss law).

($4.125\,cm^3\,K\,mol^{-1}$, $g = 2.0$). The χT curve continuously decreased upon sample cooling, reaching a χT value of $0.25\,cm^3\,K\,mol^{-1}$ at 2 K, in agreement with antiferromagnetic interactions in the whole crystal structure. The curve of $1/\chi$ *versus* T is nonlinear (see figure 8(b) insert) and does not obey the Curie-Weiss law.

4. Conclusion

Two new Mn^{III}–Cu^{II} heterometallic aggregates, **1** and **2**, based on multidentate Schiff-base ligands have been synthesized, the first time that Schiff-base ligands have been substituted for aminoalcohol ligands in reaction with zerovalent Cu and transition metal salts. The synthesis of **1** and **2** displays a new synthetic method for construction of heterometallic aggregates based on Schiff-base ligands. Since Schiff-base ligands can be designed and synthesized in numerous structural forms, many combinations of copper powder, transition metal ions and Schiff-base ligands could produce new heterometallic compounds in this subfamily.

Supplementary materials

Crystallographic data for the structural analyses have been deposited with the Cambridge Crystallographic Data Centre, CCDC reference number 661919 and 661920 for **1** and **2**, respectively. These data can be obtained free of charge at www.ccdc.cam.ac.uk/conts/retrieving.html (or from the Cambridge Crystallographic 170 Data Centre, 12 Union Road, Cambridge CB2 1EZ, UK; Fax: +44-1223/336-033; Email: deposit@ccdc.cam.ac.uk).

Acknowledgements

This work was supported by the National Science Foundation of China (No. 20701005/20701006), the Science and Technology Development Project

Foundation of Jilin Province (No. 20060420), the Postdoctoral Station Foundation of Ministry of Education (No. 20060200002), Science Foundation for Young Teachers of Northeast Normal University (No. 20070302 and 20070312) and the Testing Foundation of Northeast Normal University.

References

[1] (a) R. Sessoli, D. Gatteschi, A. Caneschi, M.A. Novak. *Nature*, **365**, 141 (1993); (b) A.J. Tasiopoulos, A. Vinslava, W. Wernsdorfer, K.A. Abboud, G. Christou. *Angew. Chem. Int. Ed.*, **43**, 2117 (2004); (c) V.M. Mereacre, A.M. Ako, R. Clérac, W. Wernsdorfer, G. Filoti, J. Bartolomé, C.E. Anson, A.K. Powell. *J. Am. Chem. Soc.*, **129**, 9248 (2007).
[2] (a) D.E. Katsoulis. *Chem. Rev.*, **98**, 359 (1998); (b) K.L. Taft, G.C. Papaefthymiou, S.J. Lippard. *Science*, **259**, 1302 (1993); (c) V.K. Yachandra, K. Sauer, M.P. Klein. *Chem. Rev.*, **96**, 2927 (1996).
[3] (a) E.C. Yang, C. Kirman, J. Lawrence, L.N. Zakharov, A.L. Rheingold, S. Hill, D.N. Hendrickson. *Inorg. Chem.*, **44**, 3827 (2005); (b) P.L. Feng, C.C. Beedle, W. Wernsdorfer, C. Koo, M. Nakano, S. Hill, D.N. Hendrickson. *Inorg. Chem.*, **46**, 8126 (2007).
[4] (a) H. Oshio, M. Nihei, A. Yoshida, H. Nojiri, M. Nakano, A. Yamaguchi, Y. Karaki, H. Ishimoto. *Chem. Eur. J.*, **11**, 843 (2004); (b) H. Oshio, N. Hoshino, T. Ito, M. Nakano. *J. Am. Chem. Soc.*, **126**, 8805 (2004); (c) H. Oshio, M. Nakano. *Chem. Eur. J.*, **11**, 5178 (2005); (d) M. Nihei, A. Yoshida, S. Koizumi, H. Oshio. *Polyhedron*, **26**, 1997 (2007).
[5] Y. Sunatsuki, H. Shimada, T. Matsuo, M. Nakamura, F. Kai, N. Matsumoto, N. Re. *Inorg. Chem.*, **37**, 5566 (1998).
[6] (a). H. Miyasaka, T. Nezu, K. Sugimoto, K. Sugiura, M. Yamashita, R. Clérac. *Chem. Eur. J.*, **11**, 1592 (2005); (b) R. Clérac, H. Miyasaka, M. Yamashita, C. Coulon. *J. Am. Chem. Soc.*, **124**, 12837 (2002).
[7] S.R. Parsons, L.K. Thompson, S.K. Dey, C. Wilson, J.A.K. Howard. *Inorg. Chem.*, **45**, 8832 (2006).
[8] P. Chaudhuri, T. Weyhermuller, R. Wagner, S. Khanra, B. Biswas, E. Bothe, E. Bill. *Inorg. Chem.*, 10.1021/ic701073j.
[9] (a) V.G. Makhankova, O.Y. Vassilyeva, V.N. Kokozay, B.W. Skelton, J. Reedijk, G. Van Albada, A.L. Sorace, D. Gatteschi. *New J. Chem.*, **25**, 685 (2001); (b) V.G. Makhankova, O.Y. Vassilyeva, V.N. Kokozay, J. Reedijk, G.A. Van Albada, J. Jezierska, B.W. Skelton. *Eur. J. Inorg. Chem.*, 2163 (2002).
[10] W.G. Wang, A. Zhou, W.X. Zhang, M.L. Tong, X.M. Chen, M. Nakano, C.C. Beedle, D.N. Hendrickson. *J. Am. Chem. Soc.*, **129**, 1014 (2007).
[11] (a) B.J. Kennedy, K. Murray. *Inorg. Chem.*, **24**, 1552 (1985); (b) E.A. Boudreaux, L.N. Mulay. *Theory and Applications of Molecular Paramagnetism*, John Wiley and Sons, New York, p 491 (1985).
[12] (a) G.M. Sheldrick. *SHELXL*97, *Program for Crystal Structure Refinement*, University of Göttingen, Göttingen, Germany (1997); (b) G.M. Sheldrick. *SHELXS*97, *Program for Crystal Structure Solution*, University of Göttingen, Göttingen, Germany (1997).
[13] I.D. Brown, D. Altermatt. *Acta Cryst.*, **B 41**, 244 (1985).
[14] (a) M. Nihei, N. Hoshino, T. Ito, H. Oshio. *Polyhedron*, **22**, 2359 (2003); (b) R.W. Saalfrank, C. Schmidt, H. Maid, F. Hampel, W. Bauer, A. Scheurer. *Angew. Chem. Int. Ed.*, **45**, 315 (2006); (c) L. Walz, H. Paulus, W. Haase, H. Langhof, F. Nepveu, *J. Chem. Soc., Dalton Trans.*, 657 (1983).
[15] (a) H. Tokoro, S. Ohkoshi, T. Matsuda, K. Hashimoto. *Inorg. Chem.*, **43**, 5231 (2004); (b) S. González, M. Pérez, M. Barrera, A.R. González Elipe, R.M. Souto. *J. Phys. Chem. B*, **102**, 5483 (1998).